Journal of Beijing Institute of Technology, 2021, Vol. 30, Suppl.1

Dynamic State Estimation for Power System with Communication Constraint Using Event-Triggered Cubature Kalman Filter

Minfeng Wei[1,2,3], Min Xu[2,3] and Fengdi Zhang[2,3,✉]

(1. School of Automation and Key Laboratory for Intelligent Control and Decision on Complex Systems, Beijing Institute of Technology, Beijing 100081, China; 2. Beijing Aerospace Automatic Control Institute, Beijing 100854, China; 3. National Key Laboratory of Science and Technology on Aerospace Intelligence Control, Beijing 100854, China)

Abstract: Accurate dynamic state estimation plays an important role in power systems. Although various filtering algorithms, such as unscented Kalman filter (UKF) and particle filter (PF), have been proposed based on phasor measurement units (PMUs), they occupy a huge communication bandwidth without specific concern, which puts heavy burden on the communication network especially when wireless communications are widely applied in smart grids. In order to relieve this communication burden, the event-triggered cubature Kalman filter (ETCKF) is proposed based on the stochastic event-triggered schedule in this paper, which guarantees that only the measurements containing innovational information are transmitted and has advantages over other event-triggered schedules, such as the deterministic event-triggered schedule, since it can maintain the Gaussian property of the conditional distribution of the system state. Based on the developed nonlinear event-triggered schedule, the cubature Kalman filter (CKF), using the third-degree spherical-radial cubature rule, further provides more accurate estimation than UKF and has lower computational complexity than PF. The proposed filter can effectively reduce the communication rate while ensuring the accuracy of filtering. Finally, the standard IEEE 39-bus system is utilized to verify the feasibility and performance of the proposed method.

Key words: event-triggered cubature Kalman filter (ETCKF); stochastic event-triggered schedule; dynamic state estimation; communication rate; phasor measurement units (PMUs)

CLC number: TP2 **Document code:** A **Article ID:** 1004-0579(2021)S1-0129-12

In the past decades, the deep penetration of renewable energy, such as wind and solar, has been urging to cut the emission from fossil fuel consumption as a green replacement. In view of power systems, it becomes more challenging to ensure the reliability and sustainability of the power grid infrastructure[1]. The energy management systems (EMSs) plays an important role to meet the challenges, which can monitor, protect and control the generation units and transmission systems[2-4]. However, because of the slow update rates of the supervisory control and data acquisition (SCADA) systems, the traditional EMSs are only effective for the steady state system model so that they cannot capture the dynamics of power systems precisely. Although static state estimation is important for power systems, it is inadequate for system monitoring especially when it comes to the employment of renewable energy. The emerge of the phasor measurement units (PMUs) based wide-area measurement system (WAMS) makes the dynamic state estimating feasible[5-7].

Received 2020-01-09
✉ Author for correspondence, Ph. D.
E-mail: 18811789446@163.com
DOI: 10.15918/j.jbit1004-0579.20003

The overview of the estimation system for a conventional power system is shown in Fig. 1. By using the global positioning system (GPS) for synchronization, the PMUs can supply measurement of voltage and current phasors at a high rate of up to 120 samples/s[4]. The measurement data collected by PMUs is sent to the phasor data concentrators (PDC), and then combined by the WAMS, finally sent to the control center through communication system for data processing in order to monitor, operate, control and protect power systems[8-9]. Among the applications performed in the control center, the DSE plays a fundamental but very critical role. So recent research effort has been concentrated on the DSE, which is essentially the real-time wide-area monitoring.

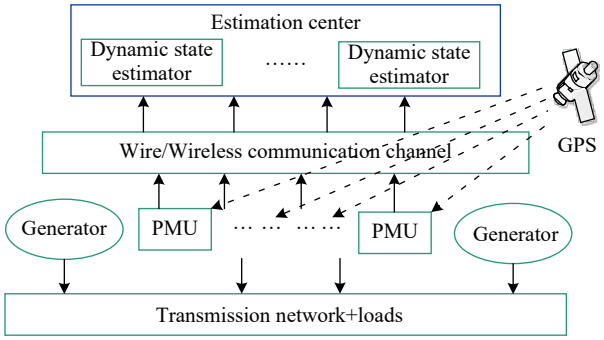

Fig. 1 System structure of estimation for WAMS consisted of PMU

Due to the nonlinearity of the power systems, different types of nonlinear filters are developed to implement the DSE, among which the most common technique is the Kalman filter (KF) based nonlinear variant[2, 7, 10-14]. Extended Kalman filter (EKF) was applied to estimate the state of power systems in Ref.[14]. However, due to the strong nonlinearity of power systems, the linear approximation of EKF became unreliable. In order to solve this problem, unscented Kalman filter (UKF) was proposed for DSE of power systems, which uses a number of points called Sigma points to approximate the expectation and covariance of random state through a nonlinear function[7]. Besides, it was shown that UKF could provide a significantly better performance than EKF even without the increase in the computational complexity. Unfortunately, UKF still has its own drawbacks such as the low numerical stability especially in the case of the large system dimension. In Ref.[12], particle filter (PF) was utilized on state estimation of power systems, and was validated on IEEE 39-bus, 10 generator system, which required huge computational resources. However, PF has practical implementation issues because of its computational complexity.

Moreover, all the filters mentioned above need PMU to transmit all measurement to DSE timely and accurately through either wired or wireless media in WAMS. However, with the widespread use of PMU, the amount of data that can be collected is enormous because the synchronized measurements can be taken at rates of about 30 to 120 samples per second[15]. It becomes difficult, actually impossible, to ensure their transmission to DSE regardless of the transmission scheme used[16-17]. The bandwidth requirements become more and more critical especially when we imagine having phasor measurement units every wherein the power grid[18]. Besides, the importance of each measurement is unequal, meaning that not all the measurement must be sent to the filter. Therefore, it is readily appreciated to seek a balance between the communication rate and estimation performance. The event-triggered schedule is an appropriate way to solve this problem. Different from the traditional sampling method, which depends on time, the event-triggered sampling schedule samples only if a certain condition, which can be called as "an event", is violated[19]. In this way, the measurements collected by the sensors can be divided into two types, the *important* ones and *useless* ones[20], only the former of which needs to be sent so that the communication rate can be remarkably reduced if the certain condition is chosen suitably. In addition, it was proved that the event-triggered sampling could get better results than the traditional sampling with the same

sampling rate[21]. Initiated by this, the event-triggered state estimation problem has been intensively studied in Refs.[22-27]. Among these, the minimum mean square error (MMSE) filter based on Kalman filter (KF) was derived in Ref.[27], which further proved that the proposed filter was superior in performance to the other kind of method with limited communication resources, i.e., KF with intermittent observations, at the same arrival rate. However, the power systems are typically nonlinear so that the linear KF-variants are infeasible. To solve this problem, this paper proposes an event-triggered nonlinear filter based on cubature Kalman filter (CKF), which is named as event-triggered cubature Kalman filter (ETCKF). From the perspective of computation, CKF is a special form of UKF but with better numerical stability and higher accuracy. Besides, the computational complexity of CKF is much less than PF, making it easier in practical engineering implementation. Therefore, the proposed ETCKF is an appropriate method to balance the communication rate and the estimation performance.

The rest of the paper is organized as follows. Section 1 introduces the theory of stochastic event-triggered schedule, which can maintain the Gaussian property of the system state 's conditional distribution. Section 2 presents the theory of CKF and finalizes the design of ETCKF. The power systems dynamics of IEEE 39-bus are presented in Section 3. A case study of the IEEE 39-bus test system is evaluated for the proposed filter in Section 4 and further compared with the CKF with intermittent observations (CKF-I) algorithm. Section 5 finally concludes the paper.

Notation $\mathbb{S}_{++}^{m}$ is the positive definite matrix. $p(\cdot)$ denotes the distribution of a random number, while the condition distribution is described as $p(\cdot|\cdot)$. $\mathcal{N}(\mu, \Sigma)$ is the Gaussian distribution with mean μ and covariance matrix Σ. $\mathbb{E}(\cdot)$ is defined as the expectation of a random variable and $\mathbb{E}(\cdot|\cdot)$ denotes the conditional expectation.

1 Stochastic Event-Triggered Schedule

After the measurement y_k is acquired, the sensor decides whether to send the data to the remote filter or not by judging the event-triggering condition. The event-triggering conditions can be generally divided into two categories, i.e., the deterministic one and stochastic one. This paper focuses on the stochastic event-triggering condition because the conditional distribution of the measurement maintains a Gaussian distribution rather than a truncated Gaussian distribution when it comes to the deterministic one[20].

Define a logic variable γ_k to indicate whether the measurement is transmitted, which can be expressed as

$$\gamma_k = \begin{cases} 1, & y_k \text{ is transferred} \\ 0, & y_k \text{ is not transferred} \end{cases} \tag{1}$$

The following rule is adopted to determine the value of γ_k: at each time instant k, an independent and identically distributed (i.i.d.) random variable η_k is generated by the event-triggered schedule, which is uniformly distributed over [0, 1]; and then, η_k is compared with the value of $\varphi(y_k, \hat{y}_{k|k-1})$, where $\varphi(y_k, \hat{y}_{k|k-1})$ is a function satisfying $\phi(y_k, \hat{y}_{k|k-1}) : \mathbb{R}^m \times \mathbb{R}^m \to [0,1]$ and $\hat{y}_{k|k-1}$ denotes the one step prediction of y_k. Therefore, if and only if $\eta_k > \varphi(y_k, \hat{y}_{k|k-1})$, the measurement y_k will be transmitted to the filter, i.e.,

$$\gamma_k = \begin{cases} 1, & \eta_k > \varphi(y_k, \hat{y}_{k|k-1}) \\ 0, & \eta_k \le \varphi(y_k, \hat{y}_{k|k-1}) \end{cases} \tag{2}$$

As η_k is uniformly distributed over [0, 1], 1-$\varphi(y_k, \hat{y}_{k|k-1})$ can be seen as the probability when the measurements are transmitted. In Ref.[20], a feasible function of φ was proposed as

$$\varphi(y_k, \hat{y}_{k|k-1}) = \exp\left[-\frac{1}{2}(y_k - \hat{y}_{k|k-1})^{\mathrm{T}} Y (y_k - \hat{y}_{k|k-1})\right] \tag{3}$$

where $Y \in \mathbb{S}_{++}^{m}$, which is a design variable used to balance the communication rate and estimation

performance and well known by the filter in advance. From Eq. (3), it can be known that the proposed event-triggered schedule needs the feedback $y_{k|k-1}$ from the filter. Therefore, the structure of this event-triggered linear filter can be shown in Fig. 2. The information set got by the filter at time instant k is given as

$$\Im_k \triangleq \{\gamma_0, \ldots, \gamma_k, \gamma_0 y_0, \ldots, \gamma_k y_k\} \tag{4}$$

Using the event-triggered schedule mentioned above, the communication rate can be obviously reduced because only the important measurement, satisfying the event-triggering condition, is transmitted to the filter. However, the main purpose of DSE is to obtain the dynamic state accurately. Besides, considering the power systems is typically nonlinear, an accurate nonlinear filter is accordingly designed to make full use of the information contained in the event-triggering condition especially when there is no data transmission.

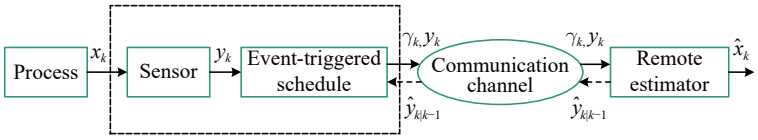

Fig. 2 Structure of the event-triggered linear filter

2 Event-Triggered Cubature Kalman Filter

The objective of the prior event-triggered schedule is to reduce the communication bandwidth between the sensor and filter. Further considering that the power systems is nonlinear, a CKF based nonlinear filter using event-triggered schedule as the sampling strategy, called as ETCKF, is developed in this section to relieve the communication burden and guarantee the accurate filtering performance. The ETCKF theory consists of the event-triggered schedule and a modified CKF algorithm. The overall framework of ETCKF is shown in Fig. 3. This section firstly introduces the original CKF and then proposes the ETCKF. Finally, the ETCKF is compared with the CKF-I, which can also reduce the communication rate.

At first, it is assumed that the power system is represented as a general discrete-time nonlinear system as follows

$$x_{k+1} = f(x_k, u_k) + v_k \tag{5}$$

$$y_k = h(x_k, u_k, v_k) + \omega_k \tag{6}$$

where $f(\cdot)$ and $h(\cdot)$ are two nonlinear functions which are known, $x_k \in \mathbb{R}^n$, $y_k \in \mathbb{R}^m$, $u_k \in \mathbb{R}^p$, $v_k \in \mathbb{R}^n$ and $\omega_k \in \mathbb{R}^m$ denote the state, the measurement, the system input, the process noise and measurement noise at time instant k respectively. It is assumed that x_0, v_k and ω_k are all white Gaussian noise with the covariance matrices $R_0>0$, $Q>0$ and $R>0$, respectively. Furthermore, x_0, v_k and ω_k are independent with each other.

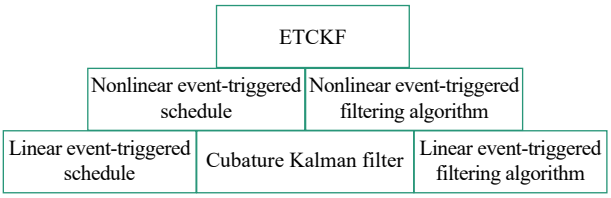

Fig. 3 Framework of ETCKF theory

2.1 Cubature Kalman filter

CKF is also based on sigma points like UKF, but it uses the third-degree spherical-radial cubature rule[28] to compute multivariate moment integrals encountered in nonlinear Bayesian filter, which makes the computation more accurate and have better numerical stability than UKF[29].

Considering the nonlinear system given by Eqs. (5) (6), it is assumed that the predictive density $p(x_k|\Im_{k-1})$ and the filter likelihood density $p(y_k|\Im_k)$ are both Gaussian, i.e., $p(x_k|\Im_{k-1}) = N(x_k|\hat{x}_{k|k-1}, P_{k|k-1})$ and $p(y_k|\Im_k) = N(y_k|\hat{y}_{k|k-1}, P_{yk})$, which eventually result in a Gaussian posterior density $p(x_k|\Im_k) = N(x_k|\hat{x}_k, P_k)$. Based on

this assumption, the Bayesian filter was proposed in Ref.[30].

Our interest of the Bayesian filter focuses on the approximation of the Gaussian integrals of the form shown as

$$\begin{aligned}&\int g(x)N(x|\hat{x},P)\,\mathrm{d}x=\frac{1}{(2\pi)^{n/2}|P|^{1/2}}\times\\&\int g(x)\exp\left[-\frac{1}{2}(x-\hat{x}^{\mathrm{T}})P^{-1}(x-\hat{x})\right]\mathrm{d}x\end{aligned}\tag{7}$$

where $g(x)$ is an arbitrary function.

In Ref.[28], the third-degree spherical-radial cubature rule was proposed to calculate (7) as follows

1) Generate the unit sigma points as

$$\xi^{(i)}=\begin{cases}\sqrt{n}\mathrm{e}_i, & i=1,\cdots,n\\ -\sqrt{n}\mathrm{e}_{i-n}, & i=n+1,\cdots,2n\end{cases}\tag{8}$$

where e_i denotes a unit vector in the direction of the coordinate axis i.

2) Compute the integral as

$$\int g(x)\,N(x|\hat{x},P)\,\mathrm{d}x=\frac{1}{2n}\sum_{i=1}^{2n}f\left(\hat{x}+\sqrt{P}\xi^{(i)}\right)\tag{9}$$

where $\sqrt{P}$ is a matrix square root satisfying $P=\sqrt{P}\sqrt{P}^{\mathrm{T}}$.

By substituting (9) into the Bayesian filter, CKF is obtained.

2.2 Event-triggered cubature Kalman filter

Based on the event-triggered schedule mentioned in Section 1 and KF, a linear MMSE filter was proposed in Ref.[20]. The proposed event-triggered linear filter can effectively balance the communication rate and estimation performance for a linear system, but it is inapplicable for the power systems due to the strong nonlinearity of the system. To utilize the benefits of the event-triggered schedule in power systems and ensure the filtering accuracy, an event-triggered nonlinear filter based on CKF is proposed in this section.

As mentioned in Section 1, all the information sent to the filter at time instant k is contained in the set $\Im_k$. For convenience, the one step state prediction and the error covariance matrix for the prediction of the states at time k are defined as $\hat{x}_{k|k-1}=\mathbb{E}(x_k|\Im_{k-1})$ and $P_{k|k-1}=\mathrm{Cov}(x_k|\Im_{k-1})$, while $\hat{x}_k=\mathbb{E}(x_k|\Im_k)$ and $P_k=\mathrm{Cov}(x_k|\Im_k)$ denote the estimation and the error covariance matrix for the estimation of x_k, respectively. Similar to the event-triggered linear filter proposed in Ref.[20], the ETCKF performs the original CKF as shown below when $\gamma_k=1$, which means that the measurement y_k is sent to the filter.

- Time update

$$\begin{aligned}\chi_{k-1}^{(i)}&=\hat{x}_{k-1}+\sqrt{P_{k-1}}\xi^{(i)},\ i=1,\ldots,2n\\ \chi_k^{(i)}&=f\left(\chi_{k-1}^{(i)},u_{k-1}\right),\ i=1,\cdots,2n\\ \widehat{x}_{k|k-1}&=\frac{1}{2n}\sum_{i=1}^{2n}\widehat{\chi}_k^{(i)}\\ P_{k|k-1}&=\frac{1}{2n}\sum_{i=1}^{2n}(\hat{\chi}_k^{(i)}-\hat{x}_{k|k-1})(\hat{\chi}_k^{(i)}-\hat{x}_{k|k-1})^{\mathrm{T}}+Q_{k-1}\end{aligned}\tag{10}$$

where $\chi_{k-1}^{(i)}$ denotes the sigma points and $\xi^{(i)}$ is shown as (8).

- Measurement update

$$\begin{aligned}\chi_{k|k-1}^{(i)}&=\widehat{x}_{k|k-1}+\sqrt{\widehat{P}_{k|k-1}}\xi^{(i)},\ i=1,\ldots,2n\\ \hat{y}_k^{(i)}&=h\left(\chi_{k|k-1}^{(i)},u_k\right),\ i=1,\ldots,2n\\ \widehat{y}_{k|k-1}&=\frac{1}{2n}\sum_{i=1}^{2n}\widehat{y}_k^{(i)}\\ P_{yk}&=\frac{1}{2n}\sum_{i=1}^{2n}(\hat{y}_k^{(i)}-\hat{y}_{k|k-1})(\hat{y}_k^{(i)}-\hat{y}_{k|k-1})^{\mathrm{T}}+R_k\\ P_{x_ky_k}&=\frac{1}{2n}\sum_{i=1}^{2n}\left(\chi_{k|k-1}^{(i)}-\hat{x}_{k|k-1}\right)(\hat{y}_k^{(i)}-\hat{y}_{k|k-1})^{\mathrm{T}}\\ K_k&=P_{x_ky_k}P_{y_k}^{\mathrm{T}}\\ \hat{x}_k&=\hat{x}_{k|k-1}+K_k\left[y_k-\hat{y}_{k|k-1}\right]\\ P_k&=P_{k|k-1}-K_kP_{yk}K_k^{\mathrm{T}}\end{aligned}\tag{11}$$

where P_{y_k} is the predicted covariance of the measurement, $P_{x_ky_k}$ is the cross-covariance of the state and the measurement and K_k is the filter gain.

However, when it comes to $\gamma=0$, the first step, i.e., Time Update, is identical to the original CKF. But in order to utilize the information implicitly provided by the event-triggering condition at the no-event instants, the design variable Y is introduced into the predicted covariance of

the measurement P_{y_k} and the one step prediction $\hat{x}_{k|k-1}$ is taken as the estimation $\hat{x}_k$.

$$P_{y_k}=\frac{1}{2n}\sum_{i=1}^{2n}(\hat{y}_k^{(i)}-\hat{y}_{k|k-1})(\hat{y}_k^{(i)}-\hat{y}_{k|k-1})^{\mathrm{T}}+R_k+Y^{-1} \tag{12}$$

$$\hat{x}_k=\hat{x}_{k|k-1} \tag{13}$$

In this way, the designed ETCKF synthesizes the advantages of event-triggered schedule and CKF, making it feasible to reduce the communication rate while ensuring the filtering accuracy.

As mentioned in Section 1, the event-triggered schedule needs data return from the filter, which will increase the communication burden. Therefore, in order to further decrease the communication rate, the sensor is equipped with a local filter which only provides the measurement prediction $\hat{y}_{k|k-1}$ for the event-triggered schedule to evaluate the event-triggered condition while the remote uses the algorithm of ETCKF. In this way, the returned data $\hat{y}_{k|k-1}$ can be gotten from the local filter rather than transmitted from the remote one. Thus, the structure of the ETCKF is designed as Fig. 4.

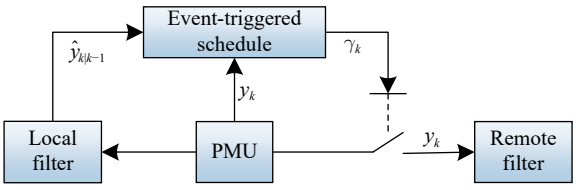

Fig. 4 System structure of ETCKF

Finally, the design of ETCKF is completed and the detail of the ETCKF algorithm is shown in Algorithm 1.

Algorithm 1 Filtering algorithm of ETCKF

Input: Information set $\Im_k$ and the point of the system u_k.

Output: Estimation results $\hat{x}_k$, P_k.

Initialisation:

Set the value of Y, the initial state x_0 and the initial errorcovariance matrix R_0.

Loop Process:

While $k\geqq 1$ **do**

if k=1 **then**

Generate sigma points $\chi_0^{(i)}$ from the distribution $N(x_0, R_0)$ according to (10).

else

Generate sigma points $\chi_{k-1}^{(i)}$ from the distribution $N(x_{k-1}, R_{k-1})$ according to (10).

end if

Calculate the one step prediction of measurement $\hat{y}_{k|k-1}$ according to (11) by the local filter, then compute γ_k by (2) and (3)

if $\gamma_1=1$ **then**

The sensor sends the measurement y_k to the remote filter. The estimation results $\hat{x}_k$ and P_k are calculated according to (11) by the remote filter.

else if γ_1= 0 **then**

The remote filter calculates $\hat{x}_k$ and P_k without the measurement value y_k but using the trigger condition. $\hat{x}_k$ and P_k are gotten by replacing the $\hat{x}_k$ and P_k are in (11) with (12) and (13).

end if

end while

2.3 Comparison with intermittent observations

The easiest way to design the event-triggered filter is to ignore the information contained in the event-triggering condition when there is no data transmission, i.e., $\gamma=0$. In this way, the designed filter simply has a degraded structure as the CKF with intermittent observations.

In other words, when $\gamma=1$, the original CKF is performed same as the ETCKF. However when it comes to $\gamma=0$, the filter only performs the time update step as (10) and takes the one step prediction and error covariance matrix for the prediction of the states as the estimation and the error covariance matrix as

$$\begin{aligned}\hat{x}_k&=\hat{x}_{k|k-1}\\ P_k&=P_{k|k-1}\end{aligned} \tag{14}$$

By comparing (14) with (12) and (13), it is

shown that although these two filtering algorithms have the same estimation $\hat{x}_k$, the error covariance matrix P_k of the proposed ETCKF is much smaller than that of CKF-I due to the introduction of Y into the error covariance matrix of ETCKF. Therefore, ETCKF is superior in performance to CKF-I at the same communication rate although both can reduce the communication rate effectively, which will be validated in Section 4.

3 Power System Dynamics of IEEE 39-Bus

The IEEE 39-bus, 10-generator test system is taken into practical consideration for verification and shown in Fig. 5. These ten generators can be divided into three categories: type I with manual excitation system without PSS, type II with IEEE DC1A AVR without PSS and type III with IEEE ST1A AVR with PSS. The classification of generators is shown in Fig. 5. The discrete dynamic equations of power systems are applied as in Section 3 of Ref.[12]. For simplicity, only type II is taken into consideration in this paper. No matter which type it belongs to, each typical generator unit can be modeled by the following discrete dynamics[12]:

$$\begin{aligned}
E'_d(k+1) &= \frac{\Delta t}{T'_{qo}}\left(-E'_d(k)+\left(X_q-X'_q\right)i_q(k)\right)+\\
&\quad E'_d(k)\\
E'_d(k+1) &= \frac{\Delta t}{T'_{do}}\left(-E'_q(k)-\left(X_d-X'_d\right)i_d(k)+\right.\\
&\quad \left.E_{fd}(k)\right)+E'_q(k)\\
\sigma(k+1) &= \Delta t\left(\eta(k)-\eta_s\right)\eta_b+\sigma(k)\\
\eta(k+1) &= \frac{\Delta t}{2H}\eta_s\left(T_m-E'_d(k)\,i_d(k)-E'_q(k)\,i_q(k)-\right.\\
&\quad \left.\left(X'_q-X'_d\right)i_d(k)\,i_q(k)-D\left(\eta(k)-\eta_s\right)\right)+\\
&\quad \eta(k)
\end{aligned} \tag{15}$$

where Δt is the sampling time, E'_d and E'_q are the transient emf of the fluxes in d-axis and q-axis, δ denotes the rotor angle, the rotor-speed is defined as η, i_d and i_q are the current flowing through generator.

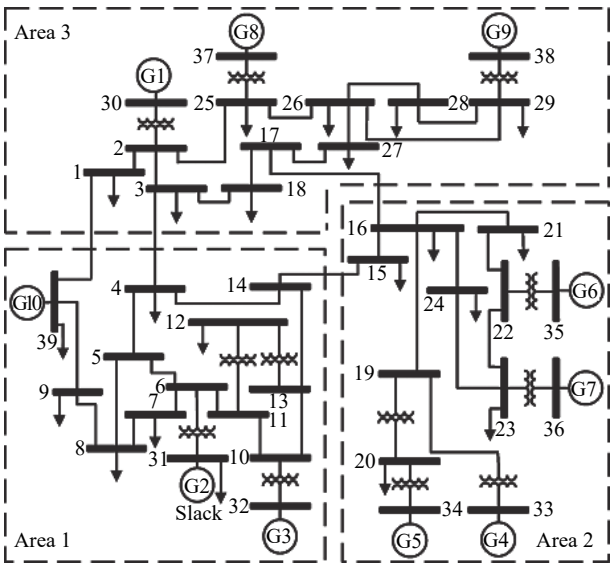

Fig. 5 IEEE 39-bus, 10-generator (New England) test system

Besides, the dynamics of the IEEE DC1A AVR without PSS is given as follows

$$\begin{aligned}
E_{fd}(k+1) &= \frac{\Delta t}{T_E}\left(-\left(K_E+A_x e^{B_x E_{fd}(k)}\right)E_{fd}(k)+\right.\\
&\quad \left.V_R(k)\right)+E_{fd}(k)\\
R_f(k+1) &= \frac{\Delta t}{T_F}\left(-R_f(k)+\frac{K_F}{T_F}E_{fd}(k)\right)+R_f(k)\\
V_R(k+1) &= \frac{\Delta t}{T_A}\left(-\frac{K_A K_F}{T_F}E_{fd}(k)-V_R(k)+\right.\\
&\quad \left.K_A R_f(k)+K_A\left(v_{ref}-v(k)\right)\right)+\\
&\quad V_R(k)
\end{aligned} \tag{16}$$

where R_f is the AVR-filter voltage, V_R denotes the AVR regulator voltage and E_{fd} is the field excitation voltage.

The measurements of the system collected by PMUs consist of the magnitude and phase for both voltage of the busbar near the generator and current flowing through generators. As we all know, the magnitude and phase of the current flowing through generators at the time instant k, i.e., $i(k)$ and $\theta_i(k)$, can be described as follows

$$\begin{aligned}
i(k) &= \sqrt{i_d^2(k)+i_q^2(k)}\\
\theta_i(k) &= \arctan\left(\frac{-i_d(k)}{i_q(k)}\right)+\delta(k)
\end{aligned} \tag{17}$$

where

$$i_d(k)=\frac{1}{X'_d}\left[E'_q(k)-\upsilon(k)\cos(\delta(k)-\theta_\upsilon(k))\right]$$
$$i_q(k)=\frac{1}{X'_q}\left[E'_d(k)-\upsilon(k)\cos(\delta(k)-\theta_\upsilon(k))\right] \tag{18}$$

where $\upsilon(k)$ and $\theta_\upsilon(k)$ denote the magnitude and phase for the voltage of the busbar near the generator, respectively, also collected by the PMU.

From Eqs. (15)–(18), it is shown that $i(k)$, $\theta_i(k)$ and the dynamic states x_{k+1} are the explicit functions of $\upsilon(k)$ and $\theta_\upsilon(k)$.

4 Simulating Results

In this section, generator 3 is used, which belongs to the type II in IEEE 39-bus 10-generator (New England) system as a typical example to verify the performance of the proposed ETCKF.

The power system dynamics of generator 3 can be rewritten as the form shown as Eqs. (5) (6), where

$$\begin{aligned}\boldsymbol{x}&=\left[E'_d\ E'_q\ \delta\ \omega\ E_{fd}\ R_f\ V_R\right]^{\mathrm{T}}\\ \boldsymbol{y}&=\left[i\ \theta_{iv}\ \theta_\upsilon\right]^{\mathrm{T}}\end{aligned} \tag{19}$$

4.1 Parameter setting

As in Ref.[12], a fault on the line connecting bus 14 to bus 15, which is simply the removal of that line, is triggered at 1.5 s while the total simulation time is 15 s. The sampling time is chosen as 0.02 s. The parameters of the generator 3 are shown in Tab. 1.

Tab. 1 Parameters of generator 3

Parameter	Value	Parameter	Value
H	35.8	D	10
X_{d}	0.2495	X'_{d}	0.0531
X_{q}	0.237	X'_{q}	0.0876
T'_{do}	5.7	T'_{qo}	1.5
A_{x}	0.07	B_{x}	0.91
K_{A}	40	T_{A}	0.2
K_{E}	1	T_{E}	0.785
K_{F}	0.063	T_{F}	0.35
υ_{ref}	1.069		

Three cases are taken into consideration for comparison among CKF, ETCKF and CKF-I. It is assumed that there is no packet dropout during the communication. For CKF, all measurements are transmitted from the PMUs to the filter while the filtering algorithm (10) and (11) is used. It is therefore considered to provide an optimal performance reference of filtering with full communication capability. The second case tests ETCKF proposed in this paper, which can significantly reduce the communication rate while still ensuring the filter quality. The third one is CKF-I, which can also decrease the communication rate by using a Bernoulli process with the given arrival rate to determine whether to transfer the measurement to the remote filter. Moreover, the remote filter performs the algorithm as mentioned in Section III-C.

In each case, the system noise is set as Gaussian noise with the covariance matrix $\boldsymbol{Q}=\mathrm{diag}[10^{-3}, 10^{-3}, 10^{-7}, 10^{-7}, 10^{-7}, 10^{-7}, 10^{-7}]$ and the observation noise is also set as Gaussian noise with the covariance matrix $\boldsymbol{R}=\mathrm{diag}[10^{-2}, 10^{-2}, 10^{-2}, 10^{-2}]$.

4.2 Dynamic performance under various communication rate

The dynamic performance of the filter under $Y=1.9I$, where $I\in\mathbb{R}^{m\times m}$ denotes the unit matrix, is shown in Fig. 6 and Fig. 7 demonstrates the comparison with $Y=0.2I$. The last two sub-figures in both Fig. 6 and Fig. 7 indicate the value of γ of ETCKF and CKF-I in each simulation time, from which it is shown that the communication rates of ETCKF are 49.6% and 20.3% for different Y respectively while those of CKF-I are 50.5% and 20.7%. In Fig. 6, it is shown that CKF and ETCKF have almost identical quality while ETCKF effectively reduces the data transmission by almost 55% because ETCKF makes full use of the information contained in the event-triggering condition (3) even when there is no information transfer. But for CKF-I, although the overall performance is

good, it still decays at a fraction of time intervals. In the case of $Y = 0.2I$, although ETCKF further reduces the data transmission by almost 80%, its estimation results demonstrate that it still can closely approximate the state of system despite of some loss of accuracy, while the performance of CKF-I is unacceptable as shown in Fig. 7. By comparing these two cases, we can conclude that with the decrease of Y, the communication rate accordingly decreases and the filtering accuracy suffers because of the non-triggered observations. But the proposed ETCKF can still get better estimation results than CKF-I under the same communication rate by two reasons. On the one hand, the event-triggered schedule only sends the important measurements to the filter. On the other hand, the filtering algorithm takes advantage of the information contained in the event-triggered schedule when there is no data transmission.

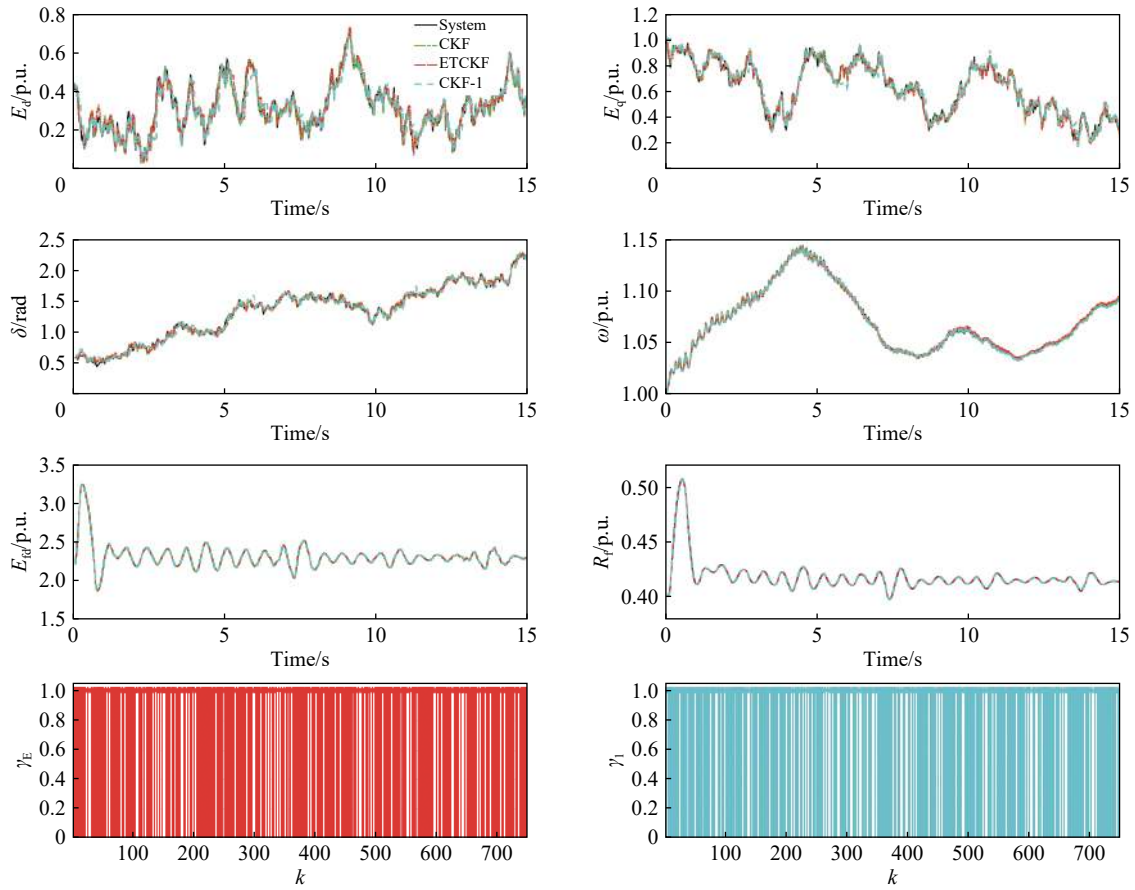

Fig. 6 States and estimation results of generator when $Y = 1.9I$

4.3 Effect of Y on static accuracy

To further demonstrate the influence of Y on the filtering accuracy, Monte Carlo simulations are carried out for 500 times, the corresponding estimation error $\|x_k - \hat{x}_k\|_2$ is shown in Fig. 8. The values of Y and the communication rate for both ETCKF and CKF-I are shown as in Fig. 8.

In Fig. 8, it is shown that the performances of both ETCKF and CKF-I are almost identical to the CKF when $Y \geq 4.5I$, which indicates the communication rate $\geq 70\%$. But when Y is reduced to $1.9I$ or even smaller, the difference between ETCKF and CKF-I in the static accuracy of filtering begins to increase. The filtering results of CKF-I become unreliable while the ETCKF can still provide acceptable results when $Y = 0.55I$ (communication rate $\approx 30\%$).

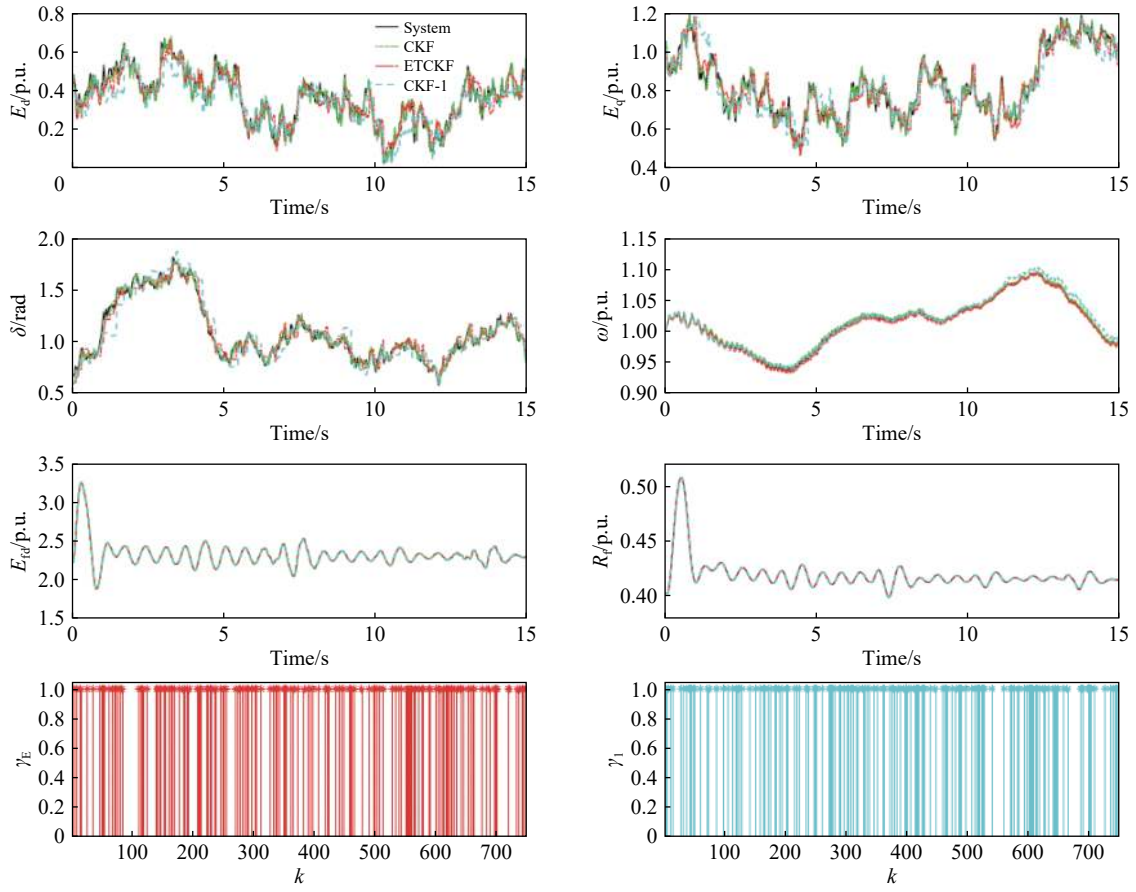

Fig. 7 States and estimation results of generator when $Y = 0.2I$

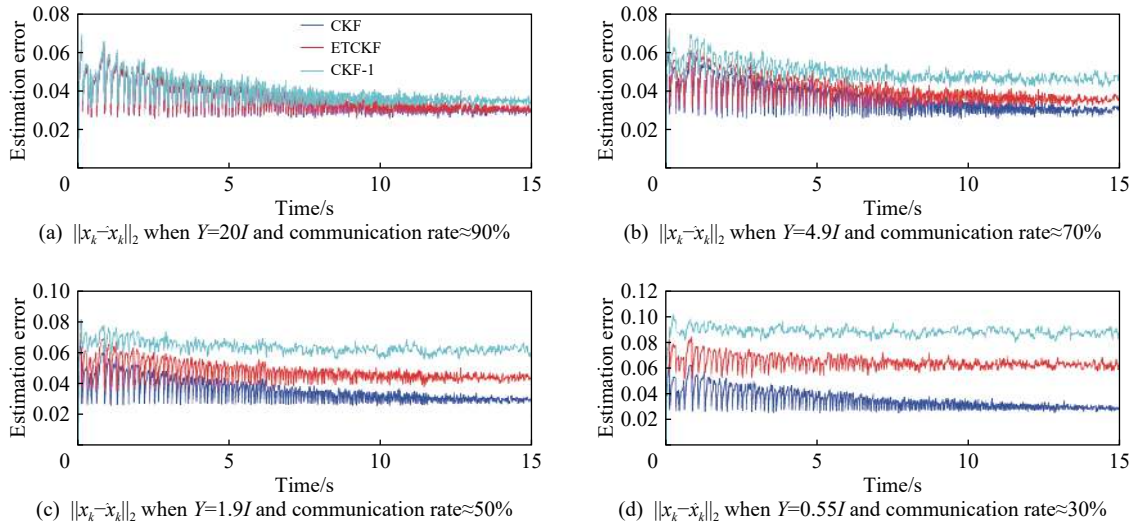

(a) $\|x_k - \hat{x}_k\|_2$ when Y=20I and communication rate≈90%

(b) $\|x_k - \hat{x}_k\|_2$ when Y=4.9I and communication rate≈70%

(c) $\|x_k - \hat{x}_k\|_2$ when Y=1.9I and communication rate≈50%

(d) $\|x_k - \hat{x}_k\|_2$ when Y=0.55I and communication rate≈30%

Fig. 8 Simulation error $\|x_k - \hat{x}_k\|_2$ for CKF, ETCKF and CKF-I under different Y and communication rate

In summary, ETCKF proposed in this paper exhibits much better performance than CKF-I. Besides, it still can provide relatively low communication rate with reliable accuracy compared with original CKF, the accuracy of which can be adjusted through Y according to the design requirement.

5 Conclusion

This paper develops a useful method for dynamic state estimation for power systems concerning communication limits, which is based on

the event-triggered schedule and CKF. The proposed ETCKF firstly introduces the stochastic event-triggered schedule to relieve the information transmission of smart grid networking. The event-triggered schedule is designed to satisfy the requirement of communication rate reduction because it ensures that only the observations containing innovational information are transmitted. Based on these innovational information, the nonlinear filter, CKF, provides accurate filtering quality with acceptable computational complexity. Therefore, ETCKF is capable of relieving communication burden while ensuring filtering accuracy. This practical design is verified on IEEE 39-bus system. Simulation results show that the proposed ETCKF is superior to CKF-I, which can not only relieve communication burden but also provide accurate filtering even at the same communication rate. With Y properly chosen, the filtering quality and communication rate can be well balanced and achieved.

References:

[1] Su W, Wang J, Roh J. Stochastic energy scheduling in microgrids with intermittent renewable energy resources [J]. IEEE Trans Smart Grid, 2014, 5(4): 1876-1883.

[2] Zhao J, Zhang G, Das K, et al. Power system real-time monitoring by using PMU-based robust state estimation method [J]. IEEE Trans Smart Grid, 2015, 7(1): 300-309.

[3] Ghahremani E, Kamwa I. Local and wide-area PMU-based decentralized dynamic state estimation in multi-machine power systems [J]. IEEE Trans Power Syst, 2016, 31(1): 547-562.

[4] Emami K, Fernando T, Iu H H C, et al. Application of unscented transform in frequency control of a complex power system using noisy PMU data [J]. IEEE Trans Ind Informat, 2016, 12(2): 853-863.

[5] Zhao M, Abur A. Multi area state estimation using synchronized phasor measurements [J]. IEEE Transactions on Power Systems, 2005, 20(2): 611-617.

[6] Gharban C K, Cory B J. Non-linear dynamic power system state estimation [J]. IEEE Power Eng Rev, 1986, 6(8): 54-55.

[7] Singh A K, Pal B C. Decentralized dynamic state estimation in power systems using unscented transformation [J]. IEEE Trans Power Syst, 2014, 29(2): 794-804.

[8] Shahraeini M, Javidi M H. Wide area measurement systems advanced topics in measurements [M]. Zahurul Hag. InTech, 2012.

[9] Shahraeini M, Javidi M H, Ghazizadeh M S. Comparison between communication infrastructures of centralized and decentralized wide area measurement systems [J]. IEEE Trans Smart Grid, 2011, 2(1): 206-211.

[10] Qi J, Sun K, Wang J, et al. Dynamic state estimation for multi-machine power system by unscented Kalman filter with enhanced numerical stability [J]. IEEE Trans Smart Grid, 2015, 9(2): 1-1.

[11] Wang C, Qin Z, Hou Y, et al. Multi-area dynamic state estimation with PMU measurements by an equality constrained extended kalman filter [J]. IEEE Trans Smart Grid, 2016, 9(2): 1-1.

[12] Emami K, Fernando T, C H H, et al. Particle filter approach to dynamic state estimation of generators in power systems [J]. IEEE Trans Power Syst, 2014, 30(5): 2665-2675.

[13] Zhou N, Meng D, Huang Z, et al. Dynamic state estimation of a synchronous machine using PMU data: A comparative study [J]. IEEE Trans Smart Grid, 2015, 6(1): 450-460.

[14] Ghahremani E, Kamwa I. Dynamic state estimation in power system by applying the extended kalman filter with unknown inputs to phasor measurements [J]. IEEE Trans Power Syst, 2011, 26(4): 2556-2566.

[15] Bose A. Smart transmission grid applications and their supporting infrastructure [J]. IEEE Trans Smart Grid, 2010, 1(1): 11-19.

[16] Gungor V C, Lu B, Hancke G P. Opportunities and challenges of wireless sensor networks in smart grid [J]. IEEE Trans Ind Electron, 2010, 57(10): 3557-3564.

[17] Wang S, Gao W, Wang J, et al. Synchronized sampling technology-based compensation for network effects in wams communication [J]. IEEE Trans Smart Grid, 2012, 3(2): 837-845.

[18] Kansal P, Bose A. Bandwidth and latency requirements for smart transmission grid applications [J]. IEEE Trans Smart Grid, 2012, 3(3): 1344-1352.

[19] Ho Y C, Cassandras C. A new approach to the analysis of discrete event dynamic systems [J]. Automatica, 1983, 19(2): 149-167.

[20] Han D, Mo Y, Wu J, et al. Stochastic event-triggered sensor schedule for remote state estimation [J]. IEEE Trans Autom Control, 2015, 60(10): 2661-2675.

[21] Astrom K J, Bo B. Comparison of periodic and event based sampling for first order stochastic systems[C]// Proceedings of IFAC World Congress, 1999, 11: 301-306.

[22] Imer O C, Basar T. Optimal estimation with limited measurements [J]. Int J of syst Control & Commun, 2010, 2(1): 5-29.

[23] Cogill R, Lall S, Hespanha J P. A constant factor approximation algorithm for event-based sampling[C]// American Control Conference, 2007: 305-311.

[24] Li L, Lemmon M, Wang X. Event-triggered state estimation in vector linear processes[C]// American Control Conference, 2010: 2138-2143.

[25] Trimpe S, D'Andrea R. An experimental demonstration of a distributed and event-based state estimation algorithm[C]// IFAC Proceedings Volumes, 2011, 44(1): 8811-8818.

[26] Rabi M, Moustakides G V, Baras J S. Adaptive sampling for linear state estimation [J]. SIAM J on Control & Optim, 2012, 50(2): 672-702.

[27] Wu J, Jia Q S, Johansson K H, et al. Event-based sensor data scheduling: Trade-off between communication rate and estimation quality [J]. IEEE Trans Autom Control, 2013, 58(4): 1041-1046.

[28] Lu J, Darmofal D L. Higher-dimensional integration with Gaussian weight for applications in probabilistic design [J]. SIAM J on Scientific Comput, 2004, 26(2): 613-624.

[29] Arasaratnam I, Haykin S. Cubature Kalman filters [J]. IEEE Trans Autom Control, 2009, 54(6): 1254-1269.

[30] Wu Y, Hu D, Wu M, et al. A numerical-integration perspective on Gaussian filters [J]. IEEE Trans Signal Process, 206, 54(8): 2910-2921.